Tertiary Structural Rearrangements upon Oxidation of Methionine^{145} in Calmodulin Promotes Targeted Proteasomal Degradation

Colette A. Sacksteder,* Jennifer E. Whittier,* Yijia Xiong,* Jinhui Li,* Nadezhda A. Galeva,‡ Michael E. Jacoby,* Samuel O. Purvine,† Todd D. Williams,‡ Martin C. Rechsteiner,§ Diana J. Bigelow,* and Thomas C. Squier*

*Cell Biology and Biochemistry Group, Biological Sciences Division, †William R. Wiley Environmental Molecular Sciences Laboratory, Pacific Northwest National Laboratory, Richland, Washington; ‡Mass Spectrometry Laboratory, University of Kansas, Lawrence, Kansas; and §Department of Biochemistry, University of Utah School of Medicine, Salt Lake City, Utah

ABSTRACT The selectivity underlying the recognition of oxidized calmodulin (CaM) by the 20S proteasome in complex with Hsp90 was identified using mass spectrometry. We find that degradation of oxidized CaM (CaM_{ox}) occurs in a multistep process, which involves an initial cleavage that releases a large N-terminal fragment (A^1-F^{92}) as well as multiple smaller carboxyl-terminus peptides ranging from 17 to 26 amino acids in length. These latter small peptides are enriched in methionine sulfoxides (Met(O)), suggesting a preferential degradation around Met(O) within the carboxyl-terminal domain. To confirm the specificity of CaM_{ox} degradation and to identify the structural signals underlying the preferential recognition and degradation by the proteasome/Hsp90, we have investigated how the oxidation of individual methionines affect the degradation of CaM using mutants in which all but selected methionines in CaM were substituted with leucines. Substitution of all methionines with leucines except Met^{144} and Met^{145} has no detectable effect on the structure of CaM, permitting a determination of how site-specific substitutions and the oxidation of Met^{144} and Met^{145} affects the recognition and degradation of CaM by the proteasome/Hsp90. Comparable rates of degradation are observed upon the selective oxidation of Met^{144} and Met^{145} in CaM-L7 relative to that observed upon oxidation of all nine methionines in wild-type CaM. Substitution of leucines for either Met^{144} or Met^{145} promotes a limited recognition and degradation by the proteasome that correlates with decreases in the helical content of CaM. The specific oxidation of Met^{144} has little effect on rates of proteolytic degradation by the proteasome/Hsp90 or the structure of CaM. In contrast, the specific oxidation of Met^{145} results in both large increases in the rate of degradation by the proteasome/Hsp90 and significant circular dichroic spectral shape changes that are indicative of changes in tertiary rather than secondary structure. Thus, tertiary structural changes resulting from the site-specific oxidation of a single methionine (i.e., Met^{145}) promote the degradation of CaM by the proteasome/Hsp90, suggesting a mechanism to regulate cellular metabolism through the targeted modulation of CaM abundance in response to oxidative stress.

INTRODUCTION

Calmodulin (CaM) functions as the primary calcium sensor in all eukaryotic cells through differential binding to more than 50 known target proteins, including kinases, phosphatases, channels, pumps, and transcription factors (1). After calcium activation, the spatial and temporal mobilization of CaM functions to differentially activate target proteins. Since the concentration of CaM-dependent target proteins exceeds that of cellular CaM, changes in rates of CaM degradation will have important physiological effects on the available CaM for target protein regulation (2,3). In particular, during biological aging the cellular abundance of CaM is reduced and dysfunctional oxiforms containing methionine sulfoxides accumulate, which will contribute to diminished calcium homeostasis as is observed in senescent animals (4–6). Underlying these age-dependent changes in CaM abundance may be oxidant-induced structural changes that promote the recognition and degradation of CaM and other signaling proteins by the proteasome in a ubiquitin-independent manner (7–9).

Well-documented examples of critical signaling proteins whose degradation by the proteasome occurs in a ubiquitin-independent manner despite their ubiquitylation suggest that there need not be a causal relationship between protein ubiquitination and degradation by the proteasome (10,11). Indeed, ubiquityl-CaM derivatized at Lys^{12} has been identified in cells; a corresponding ubiquitin-CaM ligase is likely to mediate this derivatization (12,13). However, ubiquitinylation does not result in the degradation of CaM by the proteasome (7,9). Rather, ubiquitinylation of CaM appears to regulate the binding and activation of CaM to target proteins (e.g., glycogen phosphorylase kinase). In contrast, the degradation of CaM has been shown to involve Hsp90, which is commonly present at nearly equimolar stoichiometries after the purification of the 20S proteasome (14). Prior measurements have demonstrated that the 20S proteasome forms a high-affinity complex with Hsp90 ($K_d <$ 100 nM), which selectively recognizes and degrades highly oxidized CaM in which all nine methionines are oxidized to their corresponding methionine sulfoxides; wild-type unoxidized CaM is not a substrate for proteasomal degradation (15). In these samples, a strong correlation was observed between the secondary structural changes of oxidized CaM and the recognition and degradation by the proteasome/Hsp90

Submitted March 29, 2006, and accepted for publication May 19, 2006.

Address reprint requests to Thomas C. Squier, Pacific Northwest National Laboratory, P.O. Box 999, Mail Stop P7-53, Richland, WA 99352. Tel.: 509-376-2218; Fax: 509-372-1632; E-mail: thomas.squier@pnl.gov.

0006-3495/06/08/1480/14 $2.00

doi: 10.1529/biophysj.106.086033

(14). What remains unclear is whether the site-specific oxidation of individual methionines within CaM affects degradation by the proteasome, or rather whether it is the accumulation of multiple methionine sulfoxides throughout the protein that permits the recognition and degradation of CaM by the proteasome/Hsp90.

To assess the possible role of individual methionines in modulating the degradation of oxidized CaM, we have reconstituted the 20S proteasome isolated from erythrocytes with Hsp90, and measured the ability of this complex to recognize and degrade both wild-type and mutant CaM constructs. After the partial oxidation of wild-type CaM, we have used mass spectrometry to measure changes in the overall extent of oxidation using intact protein MS spectra as well as changes in the extent of oxidation to Met^{144} or Met^{145} near the C-terminus through the consideration of fragment ions generated by electrospray ionization-collisionally induced dissociation (ESI-CID) (16). Complementary functional measurements have investigated the proteasome-dependent degradation of CaM mutants in which the majority of methionines within CaM are substituted with leucines, permitting the effect of structural perturbations associated with the site-specific substitution or oxidation of Met^{144} and/or Met^{145} to be investigated. Together, these results indicate that either site-directed amino-acid substitutions or the oxidation of these C-terminal methionines targets CaM for degradation by the proteasome/Hsp90.

EXPERIMENTAL PROCEDURES

Materials

Bovine brain Hsp90, MG132, HOMOPIPES, PIPES, and TRIS were purchased from Sigma (St. Louis, MO). Glycine, SDS, precast gels, and Gel Code Blue stain were obtained from Bio-Rad (Hercules, CA). Benchmark protein ladder molecular weight markers were from Life Technologies (Grand Island, NY). CaM mutants in which multiple methionines are mutated to leucines were expressed from existing clones that have been previously described (Table 1) (17).

Protein purification

CaM and bovine 20S proteasome were purified essentially as described previously (18–21). Briefly, after induction of reticulocytosis, washed red blood cells (>90% reticulocytes) were collected and lysed in 1 mM DTT.

TABLE 1 Nomenclature of CaM mutants

CaM Sample	Methionines	Leucine substitutions
Wild-type	36, 51, 71, 72, 76, 109, 124, 144, 145	none
L7	144, 145	36, 51, 71, 72, 76, 109, 124
L8-M144	144	36, 51, 71, 72, 76, 109, 124, 145
L8-M145	145	36, 51, 71, 72, 76, 109, 124, 144
L9	none	36, 51, 71, 72, 76, 109, 124, 144, 145

Positions of methionines and their associated site-directed leucine substitutions for wild-type CaM and indicated CaM mutants.

No detergents were added at any time during the preparation. After centrifugation (100,000 × *g*) for 90 min, glycerol was added (20% v/v) and the lysates were loaded onto a TSK-DEAE column equilibrated in 10 mM Tris-HCl (pH 7.0), 1 mM DTT, and 20% glycerol. The column was extensively washed; first overnight with 10 mM Tris-HCl (pH 7.0), 25 mM KCl, 10 mM NaCl, 1.1 mM $MgCl_2$, 0.1 mM EDTA, 1 mM DTT, and 20% glycerol (TSDG buffer); and second with TSDG buffer containing 0.1 M KCl. The 20S proteasome was then eluted using a KCl gradient between 175 and 195 mM KCl and was concentrated after ultracentrifugation and sucrose gradient purification by spinning through a Centricon-30 microconcentrator (Amicon, Danvers, MA). Isolated 20S proteasome contained no contaminating proteins visible by SDS-PAGE, and the purified 20S proteasome was shown to be free of Hsp90 by Western immunoblotting and had no intrinsic ability to degrade oxidized CaM (15,20). Protein concentration was measured using a micro-BCA assay reagent kit (Pierce, Rockford, IL) using either CaM or bovine serum albumin as protein standards. In the case of the CaM protein standard, the concentration was determined using the published molar extinction coefficient ($\in_{277nm}$ = 3029 M^{-1} cm^{-1}) for calcium-saturated CaM (22).

CaM oxidation

Methionines in wild-type or mutant CaM were oxidized to their corresponding sulfoxides (CaM_{ox}) by incubating 60 μM CaM in 50 mM HOMOPIPES (pH 5.0), 0.1M KCl, 1 mM $MgCl_2$, and 0.1 mM $CaCl_2$ with 50 mM H_2O_2 at 25°C. The concentration of H_2O_2 was determined by using the published extinction coefficient, $\in_{240nm}$ = 39.4 ± 0.2 M^{-1} cm^{-1} (23). After incubation, the reaction was stopped by dialyzing the sample against multiple changes of distilled water (3 × 5 liters) buffered with 1 mM sodium bicarbonate at 4°C. The homogeneity of oxidized samples was assessed by electrospray mass spectrometry, which demonstrated that all methionines were quantitatively oxidized (17). Partial oxidation of methionines in wild-type CaM was performed essentially as described above, except that oxidation times were limited to 1-, 2-, and 4-h timepoints; samples were pooled to enhance sample heterogeneity.

Reconstitution of 20S proteasome with Hsp90

The 20S proteasome (0.6 μM) was incubated in the absence and presence of Hsp90 (2.5 μM) at 37°C for 1 h before substrate addition, permitting an efficient functional reconstitution in 50 mM PIPES (pH 6.5), 0.1 M KCl, 10 mM $MgCl_2$, 0.1 mM EGTA (15).

CaM proteolysis by the 20S proteasome

Quantitative measurements of the rates of proteolysis using oxidized CaM as a substrate for the proteasome were routinely determined by monitoring the disappearance of the integrated intensity of CaM bands on SDS-polyacrylamide gels, as previously described (15) or from a consideration of intensity changes associated with ESI-MS measurements of intact CaM or after ESI-CID fragmentation (see below). Briefly, native or oxidized CaM (12 μM) was incubated with red blood cell 20S proteasomes (0.6 μM) in the presence of Hsp90 (2.5 μM) at 37°C in 50 mM PIPES (pH 6.5), 0.1 M KCl, 10 mM $MgCl_2$, and either 0.1 mM EGTA or 0.1 mM $CaCl_2$. At the indicated times, 40 nM MG132 was added to the reaction to inhibit the proteasome, before sample analysis.

Mass spectrometric analysis

CaM samples were injected onto the column (C_4, 5 cm × 1 mm i.d., Micro-Tech Scientific, Vista, CA) equilibrated with 40% ethanol in 0.1% aqueous TFA and eluted with a linear gradient (3% ethanol/min) developed with an Ultra Plus II MicroLC system (Micro-Tech Scientific) at a flow rate

50 μl/min. The HPLC was coupled to the electrospray source of a Q-TOF-2 mass spectrometer (Micromass, Manchester, UK). Proteins MS spectra were acquired in alternating cycles of ESI-MS over 800–3000 mass-to-charge (m/z) units and ESI-CID of the $[M+14H]^{14+}$ ion of CaM, m/z = 1195.5 with a precursor selection window of 11 u with fragment ions detected from 100 to 3000 (m/z) units. Total oxiform distribution and extent of oxidation in CaM was calculated from the charge deconvoluted ESI-MS spectra. Charge deconvolution was performed using the MaxEnt1 routine in the MassLinx 4.0 software (Micromass). The number of Met(O) was calculated and averaged over five parallel experiments. Additional information regarding the extent of oxidation association with Met^{144} and Met^{145} was measured by ESI-CID, as previously described (16).

To identify released peptides after incubation of CaM_{ox} with the proteasome, samples were injected onto a reversed-phase column (C_{18}, 5 cm × 0.32 mm i.d., Micro-Tech Scientific) at a flow rate of 10 μl/min with a linear gradient raising from 20 to 70% (v/v) methanol in 0.08% (v/v) aqueous formic acid over a period of 50 min using a Waters CapLC XE system (Waters, Manchester, UK). Analytes were directly eluted into the source of the Q-TOF-2 mass spectrometer and analyzed in a data-dependent fashion with dynamic exclusion. Precursor ions in a survey ESI-MS scan (m/z 300–2000 mass range) were selected and fragmented during ESI-MS/MS scan (m/z 100–2000 mass range). The resulting MS/MS spectra were deconvoluted using MaxEnt3 routine in the MassLinx 4.0 software (Micromass) and matched against sequences derived from nonspecific digestion of CaM.

Alternatively, CaM_{ox} was tryptically digested and submitted for LC-MS/MS analysis on a LTQ-FT instrument (ThermoFinnigan, San Jose, CA) for the identification of the oxidation states of Met^{144} and Met^{145}. The high performance liquid chromatographic separation system has been described elsewhere (24). LTQ-FT utilizes a hybrid linear quadrupole ion trap coupled to ion cyclotron resonance (ICR) mass measurement to produce isotopically resolved signatures of MS/MS fragments. This allowed for specific identification of the oxidation state associated with each of the two sequential methionines (M^{144} and M^{145}) in the C-terminal tryptic peptide of CaM. Previous LC-MS/MS analysis using an LCQ three-dimensional quadrupole ion trap instrument (ThermoFinnigan) had resulted in ambiguous data. The LTQ-FT benefits from the excellent ion control capabilities of the linear ion trap, which are coupled to the superior resolving power of the ICR. The input of potential precursor-ion mass-to-charge (m/z) candidates are provided, which are isolated in the linear trap at high ion populations and then subjected to collisionally induced fragmentation (CID). The fragment ions are then extracted into the ICR cell with m/z values measured at a resolution >50,000 (full width at half-maximum). This results in an isotopically resolved signature of the fragmentation products, which allowed specific identification of the oxidized moiety associated with the C-terminal peptide of CaM. The observed isotopic distributions of MS/MS reporter fragments were evaluated relative to their theoretical distribution using the THRASH algorithm for isotopic fitting (25) as employed by ICR-2LS software developed at PNNL (http://ncrr.pnl.gov/software/). Fit values of 0.15 and less indicate that the isotopic signature observed is valid. A value of 0.09 was obtained for the M^{145} reporter ion.

Circular dichroism measurements

Circular dichroism (CD) spectra were measured with an AVIV Model 60DS spectropolarimeter (Aviv, Lakewood, NJ) and a temperature-jacketed spectral cell with a pathlength of 0.5 cm. Spectra were recorded in 10 mM TRIS (pH 7.5), 50 mM KCl, 1 mM $MgCl_2$, and 0.1 mM $CaCl_2$ at 1-nm intervals between 202 and 240 nm. Temperature-dependent changes in the CD spectra involved three scans at each temperature with 2 min to allow equilibrium in both the forward and reverse directions. No hysteresis was observed, and reported error bars represent the standard deviation of the mean. The mean residue molar ellipticity, [P], was calculated using the formula

$$[\Theta] = \frac{\theta_{\text{measured}} \times 10^{-3}}{[P] \times n \times l},$$

where P_{measured} is the measured ellipticity in millidegrees, [P] and n are the concentration (in decimoles per cubic centimeter), and the number of peptide bonds in CaM, respectively, and l is the path length of the CD cell. The apparent α-helical content was determined using the program CONTIN in the CDPro software package (http://lamar.colostate.edu/~sreeram/CDPro/). This program determines the best fit to the data using an algorithm for comparative analysis of the measured data with a reference data set that consisted of 43 soluble proteins and 13 membrane proteins (26).

Fluorescent labeling of CaM

CaM was reacted with Alexa Fluor 532 using a protein labeling kit purchased from Molecular Probes (Eugene, OR) and separated from unreacted probe using a G-25 Sephadex column (Amersham Biosciences, Piscataway, NJ). The final molar stoichiometry was ~1 mole of fluorophore per mole of CaM.

FCS measurements

Fluorescence correlation spectra were obtained using a Nikon TE300 inverted microscope (Nikon, Tokyo, Japan) modified for these measurements, where excitation was from a Coherent Verdi laser (532 nm, Coherent, Santa Clara, CA) attenuated by a circular neutral density filter and focused by a 100× objective lens (S Fluo100, Nikon) 50 μm above the surface of the cover slide. The fluorescence was collected using the same objective, separated by a 550DCLP dichroic mirror (Chroma Technology, Brattleboro, VT). A 50 μm diameter pinhole was installed in the image plane of the output fluorescence to get rid of out-of-focus signals. To minimize the effect of after-pulse, the fluorescence was split by a cube beam splitter (Thorlabs, Newton, NJ), and detected subsequent to a HQ560 emission filter (Chroma Technology) using a pair of SPCM-AQR-14 avalanche photodiodes (Perkin-Elmer Optoelectronics, Vaudreuil, Canada). The output was fed into a Flex01-05D multi-τ correlator (Correlator.com, Bridgewater, NJ), and the fluorescence correlation function was calculated in real-time. Evaluation of the correlation curves was carried out by Origin's nonlinear fitting function (MicroCal Software, Northampton, MA), where a quantitative consideration of the sample heterogeneity is possible from a consideration of the fluorescence correlation curves associated with the fluorescence intensity traces. The correlation curve $G(\tau)$ is described by the equation

$$G(\tau) = \frac{1}{N}\frac{1}{\left(1+\frac{\tau}{\tau_D}\right).\sqrt{1+\frac{\tau}{S^2\tau_D}}}, \quad \text{where } \tau_D = \frac{\omega^2}{4D_t}.$$

Here, N is the number of molecules in the focal point, S is the ratio of half-height to radius (ω) of the focal point, τ is the lag time between fluorescence bursts, τ_D is the apparent diffusion time of the molecule, and D_t is the translational diffusion coefficient. The setup was calibrated using rhodamine 6G, whose diffusion coefficient is $2.8\times10^{-10}m^2s^{-1}$.

RESULTS

Selective degradation of more highly oxidized form of CaM by the proteasome

Hydrogen peroxide mediates the selective oxidation of methionines to their corresponding methionine sulfoxides (i.e., Met(O)) in CaM (27). After exposure of CaM to hydrogen peroxide, the extent of oxidation can be determined using mass spectrometry to measure the distribution of CaM

oxiforms. A broad distribution of CaM oxiforms is observed (Fig. 1 *A*), resulting in an average of ~2.4 methionine sulfoxides per CaM. This mixture contains both unmodified CaM with a mass of 16,706.9 ± 0.8 Da and oxiforms in which from one to five methionines are oxidized to their corresponding methionine sulfoxides (Met(O)) with respective masses of 16,723, 16,739, 16,755, 16,772, and 16,788 Da (Fig. 1 *A*). Less abundant high mass oxiforms are partially obscured by trace salts that inevitably survive desalting and were not considered in the calculations.

After incubation of oxidized CaM with the 20S proteasome reconstituted with Hsp90 (i.e., proteasome/Hsp90), MG132 was added to inhibit further degradation and ESI-MS spectra were obtained for intact CaM. Using SDS-PAGE to monitor the extent of CaM degradation, we observe that 43 ± 9% of the intact CaM band apparent at 17 kDa was digested by the proteasome (data not shown). In the absence of Hsp90, CaM is not degraded by the 20S proteasome (15), indicating that Hsp90 plays an essential role in mediating the degradation of oxidized CaM by the proteasome. Highly oxidized species are selectively degraded, as shown by the greater loss of spectral intensity corresponding to the higher oxidation states of CaM in comparison to the original distribution of CaM oxiforms before incubation with the proteasome/Hsp90 (Fig. 1 *A*). Correcting for the MS-induced loss of water (28), a consideration of the decrease in the intensity associated with each CaM oxiform reveals an approximately linear relationship between the extent of CaM degradation by the proteasome and the number of oxidized methionines (Fig. 1 *B*).

From a consideration of prior HPLC measurements in which rate constants were determined for the oxidation of methionines in different tryptic fragments of CaM, it is possible to assess potential linkages between site-specific oxidative modifications and the extent of CaM_{ox} degradation. In the case of the C-terminus tryptic peptide of CaM that contains Met^{144} and Met^{145} there is a strong correlation between the extent of Met^{144} and Met^{145} oxidation and the fraction of CaM_{ox} that is recognized and degraded by the proteasome (Fig. 1 *B*). These latter results are consistent with prior observations indicating that global conformational changes are associated with the oxidation of Met^{144}/Met^{145}, while the oxidation of the other seven methionines in CaM result in minimal structural or functional perturbations (17, 28–30). Consistent with this observation, negligible degradation is observed at low levels of oxidation (i.e., Met(O)/CaM = 1), where Met^{76} is known to be preferentially oxidized (21).

To directly measure the extent of Met^{144} and Met^{145} oxidation, and whether the oxidation of these sites promotes the recognition and degradation of CaM_{ox} by the proteasome/Hsp90, the whole protein oxiform content and extent of oxidation at Met^{144} and Met^{145} in CaM_{ox} was measured simultaneously using ESI-MS and ESI-MS/MS in alternating cycles, which has previously been shown to permit a quantitative determination of the extent of oxidation associated with peptide y_n ions that contain Met^{144} and Met^{145} and their associated oxiforms containing either one (i.e., y_n +16) or two (i.e., y_n + 32) methionine sulfoxides (16). The most abundant signals revealing oxidation were obtained

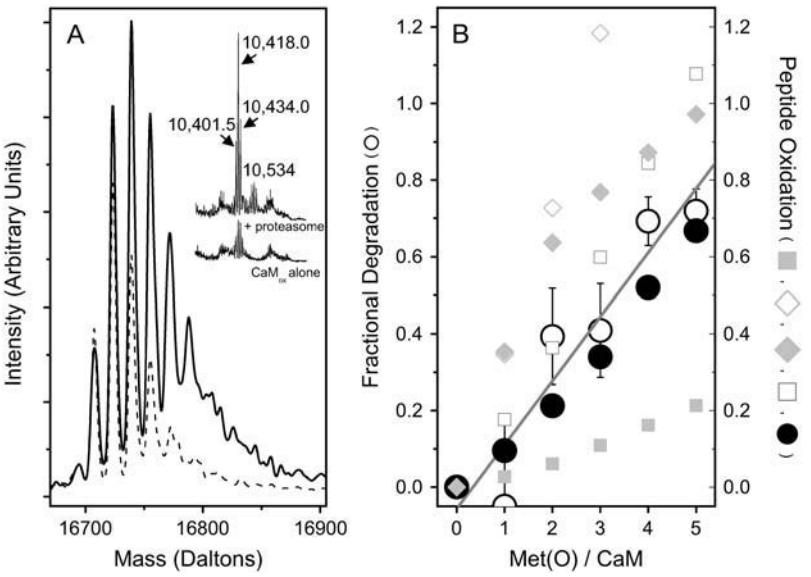

FIGURE 1 Selective degradation of oxidized CaM by the proteasome. Intact protein ESI-MS spectra of CaM, whose average extent of oxidation is 2.4 Met(O)/CaM, before (—) and after (- - -) incubation with the proteasome/Hsp90 (*A*). Major peaks correspond to CaM oxiforms with an integral number of Met(O) per CaM. Inset shows large fragment (10,401.5 Da) and two corresponding oxiforms containing one (i.e., 10,418 Da) and two (i.e., 10,434 Da) Met(O) that appear during degradation of CaM_{ox}; these represent ~40% of the ion intensity in the spectrum. The parent mass of the large fragment is 10,401.5 Da and was confidently identified to be Ala^1–Phe^{92} using the MS/MS spectra obtained from ESI-CID experiments on the $[M+9H]^{9+}$ ion (m/z = 1156.8) through assignment of a series of b_n ions (n = 2–9) as well as N-terminal internal fragments corresponding to Asp^2–Gln^3, Asp^2–Leu^4, and Asp^2–Thr^5. Panel *B* shows the extent of proteasomal degradation for each oxiform (○) and the corresponding extent of oxidation of peptides containing Met^{36} (*shaded square*); Met^{51}, Met^{71}, and Met^{72} (*open diamond*); Met^{76} (*shaded diamond*); Met^{109} and Met^{124} (*open square*); and Met^{144} and Met^{145} (*solid circle*). The percent degradation for each oxiform was determined by the difference between MS spectral peak heights in panel *A* before and after proteasome/Hsp90 incubation. The extent of oxidation for Met^{144} and Met^{145} and other methionines was calculated from measured rate constants (21). Experimental conditions involved incubation of 12 μM CaM in the presence of 0.6 μM 20S proteasome reconstituted with 2.5 μM Hsp90 for 24 h in 50 mM PIPES (pH 6.5), 0.1 M KCl, 10 mM $MgCl_2$, 2.0 mM ATP, and 0.1 mM $CaCl_2$, essentially as previously described (15). Before MS analysis the proteasome was inhibited upon addition of 40 nM MG132.

from the y_5 and y_6 ions, which permit facile visualization of the extent of oxidation at Met^{144} and Met^{145} (Fig. 2). However, equivalent results are obtained from a consideration of all detected ions (i.e., y_5, y_6, y_7, y_8, and y_9). The calculated ion intensities associated with the sum of the $y_n + 16$ and $y_n + 32$ ions represent 49 ± 1% of the total ion intensity for the peptide fragments. These results indicate that approximately one-half of these sites (i.e., Met^{144} and Met^{145}) are oxidized in CaM_{ox} to their corresponding methionine sulfoxide. Since there are ~2.4 Met(O) per CaM (Fig. 1), the oxidation of Met^{144} and/or Met^{145} represents ~20% of the total extent of oxidation, consistent with prior kinetic measurements regarding the extent of oxidation involving these sites (21).

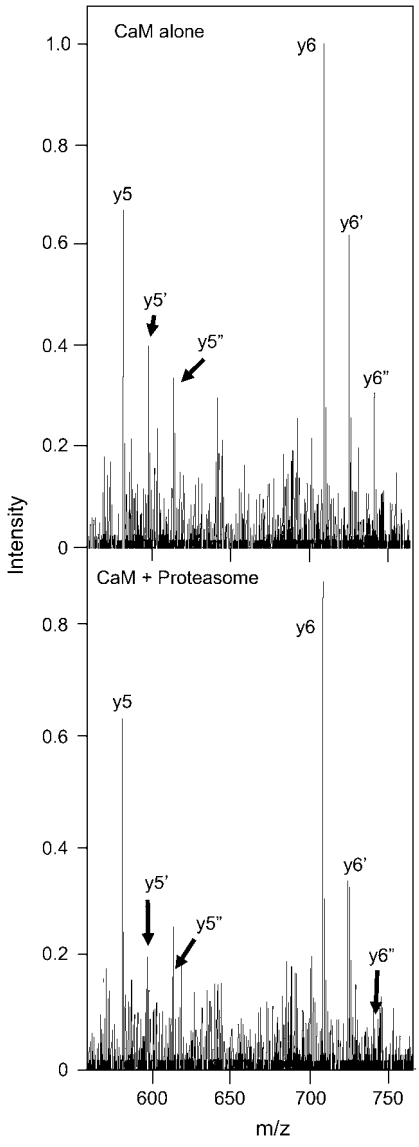

FIGURE 2 Oxidation of Met^{144}/Met^{145} results in the preferential degradation of CaM. ESI-CID MS/MS spectra before (*top*) or after (*bottom*) exposure to the proteasome obtained from the $[M+14H]^{14+}$ ion (m/z = 1195.5) for the intact protein highlighting the y_5 (M^{144}–Lys^{148}) and y_6 (Q^{143}–Lys^{148}) ions that include Met^{144} and Met^{145} and associated oxiforms (i.e., y_n+16 and y_n+32) in which one (i.e., y_5' or y_6') or both (i.e., y_5'' or y_6'') methionines are oxidized to their corresponding methionine sulfoxides. Individual ions correspond to y_5 (581.3 Da), y_5' (597.3 Da), y_5'' (613.3 Da), y_6 (709.4 Da), y_6' (725.4 Da), and y_6'' (741.3 Da).

Data regarding degradation of CaM_{ox} by the proteasome was obtained from the absolute signal intensities of the y_n ions upon incubation of CaM_{ox} with the proteasome. Addition of the proteasome results in an apparent decrease in signal intensity for all y_5 and y_6 ions (Fig. 2); however, there is a substantially greater decrease of 49 ± 3% and 59 ± 11% for the y_n+16 and y_n+32 ions, respectively, compared to an intensity decrease of 12 ± 4% for unoxidized y_n peptides. These results indicate that the oxidation of Met^{144}/Met^{145} results in the selective degradation of CaM_{ox} by the proteasome (Fig. 1), consistent with the whole protein data already described. Since equivalent extents of degradation are observed for the singly oxidized peptide (i.e., y_n+16) relative to when both Met^{144} and Met^{145} are oxidized (y_n+32), these results indicate that the oxidation of a single site (i.e., Met^{144} or Met^{145}) results in an approximate fivefold increase in the extent of degradation for CaM_{ox}.

Preferential degradation of CaM oxiforms containing $Met(O)^{144}$/ $Met(O)^{145}$

To determine whether CaM oxiforms that contain $Met(O)^{144}$ or $Met(O)^{145}$ are selectively targeted for degradation, we have used mass spectrometry to measure the peptide products resulting from the degradation of CaM_{ox} by the proteasome/Hsp90. After incubation of CaM_{ox} with the proteasome, we observe a large CaM fragment with a mass of 10,401.5 ± 0.8 Da, (see *inset* in Fig. 1 *A*). Two oxiforms of this fragment are resolved with masses of 10,418.0 and 10,434.0, which differ by 16 Da as expected for different oxiforms of CaM that contain variable numbers of Met(O). An additional minor fragment of CaM with a parent mass of 9999.0 ± 0.8 Da was also observed (data not shown). In the case of the 9999.0 ± 0.8 Da mass there was only a single candidate sequence (i.e., Ala^1–Phe^{89}) with a theoretical average mass of 9999.0 Da that was consistent with the measured mass. The mass of the larger fragment with a parent mass of 10,401.5 Da was consistent with three candidate peptides, and was confidently identified to be Ala^1–Phe^{92} using the MS/MS spectra (see legend to Fig. 1). Therefore, Ala^1–Phe^{89} and Ala^1–Phe^{92} represent two major products of proteasome degradation. The retention of an intact N-terminal domain after cleavage by the proteasome indicates that this portion of CaM_{ox} is not selectively recognized for degradation by the proteasome, consistent with the hypothesis that the oxidation of methionines near the C-terminus (i.e., Met^{144} and Met^{145}) promotes the selective recognition of CaM_{ox} for degradation by the proteasome.

MS/MS was also used to identify the CaM-derived peptides released after the digestion of CaM_{ox} by the proteasome. The majority of these peptides are derived from the C-terminal

domain of CaM; many contain Met^{144} and Met^{145}. Three abundant peptides correspond to the following sequences: Gly^{132}–Lys^{148} in which both Met^{144} and Met^{145} are oxidized (ion current = 3971), Ala^{128}–Lys^{148} in which both Met^{144} and Met^{145} are oxidized (ion current = 793), and the unoxidized peptide Glu^{123}–Lys^{148} (ion current = 1105) (Table 2). A consideration of the relative ion currents associated with peptides that contain both Met^{144} and Met^{145} provides a semiquantitative estimate of their respective abundances, and indicates that >80% of the detected peptides contain $Met(O)^{144}$ and $Met(O)^{145}$. Together, these results indicate that there is a strong propensity for degradation of CaM oxiforms that contain $Met(O)^{144}$ and/or $Met(O)^{145}$ by the proteasome, and that degradation initially proceeds in the region of $Met(O)^{144}$ and $Met(O)^{145}$ leaving the N-terminal region uncleaved.

Relative sensitivity of $Met(O)^{144}$ versus $Met(O)^{145}$ to oxidation

To distinguish the roles of Met^{144} from Met^{145} in the recognition and degradation by the proteasome/Hsp90, we have used high resolution LTQ-FTICR mass spectrometry to identify the oxidation states of Met^{144} relative to Met^{145}. CaM_{ox} was digested with trypsin and the MS fragmentation was performed for the $[M+3H]^{3+}$ ions of the peptide Glu^{127}-Lys^{148} that contains Met^{144} and Met^{145}. Three distinct oxidation states for this peptide were observed, corresponding to the unoxidized peptide (830.7 m/z), a singly oxidized peptide (836.0 m/z) containing one methionine sulfoxide, and a doubly oxidized peptide (841.4 m/z) in which both Met^{144} and Met^{145} are oxidized to their methionine sulfoxides. A comparison of the fragmentation pattern observed for the singly oxidized peptide in comparison to the unoxidized and doubly oxidized peptide indicates that Met^{145} is selectively oxidized before the oxidation of Met^{144} (Fig. 3). This is apparent from a consideration of the b_{18}^{+2} and y_4^{+1} ions, which respectively resolve the extent of oxidation of either Met^{144} or Met^{145}. Upon oxidation of both Met^{144} and Met^{145} there are 8 amu and 16 amu mass shift of the parent ions (i.e., b_{18}^{+2} and y_4^{+1} ions; Fig. 3 *A*) to form their respective oxidation products (i.e., $b_{18}^{+2'}$ and $y_4^{+1'}$ ions; Fig. 3 *B*) in which either Met^{144} or Met^{145} are oxidized to their corresponding methionine sulfoxide. Under conditions where only one methionine is oxidized in the peptide Glu^{127}–Lys^{148}, it is apparent that the ion intensities of unoxidized b_{18}^{+2} ion greatly exceed that of the ion intensity of the oxidized $b_{18}^{+2'}$ ion (Fig. 3 *D*), indicating that Met^{144} is not appreciably oxidized. In contrast, the ion intensity of unoxidized y_4 ion is negligible in comparison to the oxidized y_4' ion (Fig. 3 *C*), indicating that Met^{145} is largely oxidized to its corresponding methionine sulfoxide. This observation that Met^{145} is preferentially oxidized relative to Met^{144} is consistent with the strong correlation previously observed between surface accessibility and extent of in vitro oxidation by hydrogen peroxide, as well as prior molecular dynamics calculations that indicate the surface accessibility of Met^{145} (i.e., 25 $Å^2$) to be substantially larger than that of Met^{144} (i.e., <1 $Å^2$) in calcium-activated calmodulin (21). Thus, under mild conditions of oxidation Met^{145} is preferentially oxidized to the exclusion of Met^{144}. Since CaM_{ox} is degraded to a similar extent upon the oxidation of only one site (i.e., Met^{145}) relative to that observed upon oxidation of both Met^{144} and Met^{145} (see Fig. 2), these results strongly suggest that the oxidation of Met^{145} is sufficient for the recognition of CaM_{ox} by the proteasome for degradation.

Effects of methionine oxidation on the hydrodynamic radius of CaM

Oxidized proteins are predisposed to form aggregates, which are known to diminish rates of proteasome-dependent degradation (31,32). We have used fluorescence correlation spectroscopy to assess possible oxidation-dependent changes in the translational diffusion coefficient of CaM, which is dependent on structural changes that affect the hydrodynamic radius (33). Upon oxidation of all nine methionines in CaM there is no appreciable change in the correlation curve (Fig. 4). Fitting the data permits a determination of the translational diffusion coefficients (D_t), which were, respectively, $1.1 \times 10^{-10}\ m^2\ s^{-1}$ and $1.0 \times 10^{-10}\ m^2\ s^{-1}$ for wild-type and oxidized CaM. The expected diffusion coefficient for calcium-activated CaM is $0.9 \times 10^{-10}\ m^2\ s^{-1}$ (34), in good agreement with these measurements. The insensitivity of the diffusion coefficient upon oxidation of all nine methionines suggests that there are minimal structural changes in the hydrodynamic shape of CaM and that there is no appreciable aggregation upon oxidation of all nine methionines.

Rates of CaM degradation upon selective oxidation of Met^{144} and Met^{145}

Additional clarification of the sensitivity of CaM to degradation by the proteasome/Hsp90 was achieved by engineering a mutant CaM (i.e., CaM-L7; Table 1) in which the majority

TABLE 2 Peptide identifications after incubation of CaM_{ox} with the proteasome

Peptide sequence*	Ion current	Observed mass (Da)	Theoretical mass (Da)
D.G^{132}DGQVNYEEFVQM*M*TAK^{148}	3971	1977.9	1977.8
E.A^{128}DIDGDGQVNYEEFVQM*M*TAK^{148}	793	2392.2	2392.0
D.E^{123}MIREADIDGDGQVNYEEFVQMMTAK^{148}	1105	3018.6	3018.3

Monisotopic masses; all peptide identifications were confirmed matching Q-TOF of CID spectra to predicted fragments.
*The term *M** indicates an oxidation product with a mass of +16 Da.

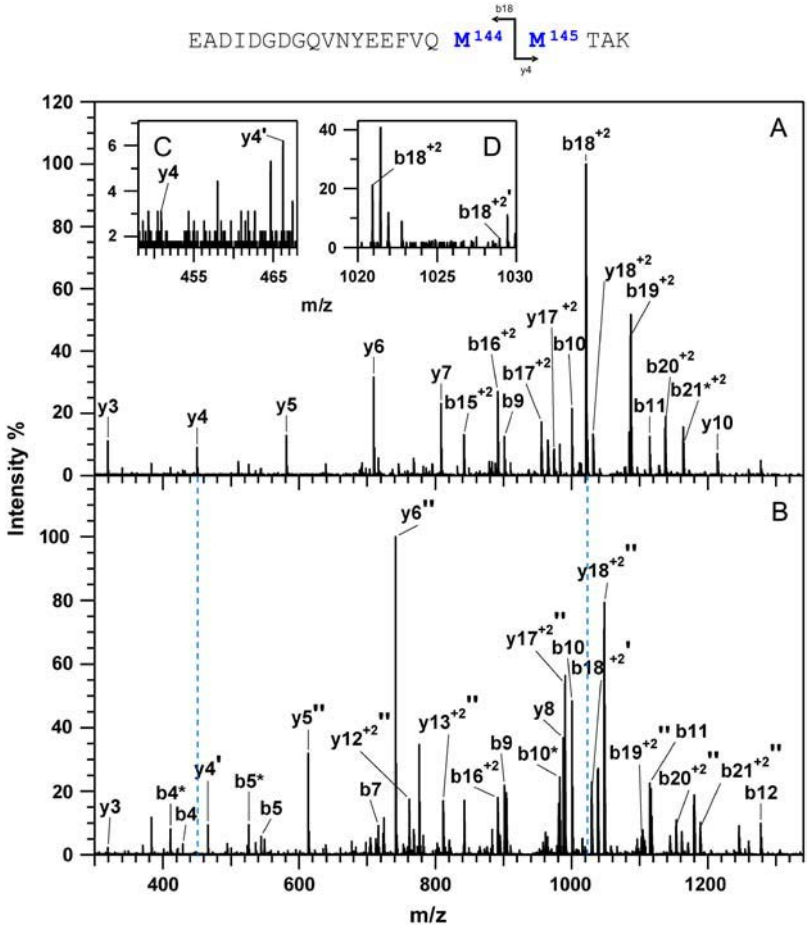

FIGURE 3 Sequential oxidation of Met^{145} before Met^{144}. MS/MS spectra for $[M+3H]^{3+}$ ions corresponding to carboxyl-terminus tryptic fragment containing Met^{144} and Met^{145} in wild-type CaM before (*A*) and after (*B*) the oxidation of both methionines, and comparison with intensities associated with the parent y_4^+ (450.2 m/z) and b_{18}^{+2} (1020.0 m/z) ions and their oxidized products (i.e., $y_4^{+'}$ at 466.2 m/z and $b_{18}^{+2'}$ at 1028.9 m/z) for the peptide containing a single methionine sulfoxide, which are respectively shown in panels *C* and *D*. Positions of parent unoxidized peptides (i.e., y_4^+ and b_{18}^{+2}) are highlighted with vertical dashed blue lines in panel *B*. In all cases, ions containing one and two methionine sulfoxides are respectively designated with either a single or double prime; ions minus a water molecule are designated with asterisks (e.g., b_4* and b_5* in *B*).

of methionines are substituted with leucines, permitting the specific oxidation of Met^{144} and Met^{145}. The tertiary structures of wild-type CaM and CaM-L7 have previously been shown to be virtually identical, and CaM-L7 fully activates target proteins (17,35,36). Using SDS-PAGE and gel densitometry to measure the rate of CaM degradation by the proteasome/Hsp90, we find that, after the oxidation of Met^{144} and Met^{145} in CaM-$L7_{ox}$, that the rate of CaM degradation by the proteasome is comparable to that observed for wild-type CaM_{ox} in which all nine methionines are oxidized under conditions of low calcium (Fig. 5). Consistent with the stabilization of the tertiary structure of CaM by calcium binding (14), the rate of proteasome degradation is diminished somewhat in the presence of 0.1 mM calcium for wild-type and more extensively for L7-CaM_{ox}. These results suggest that the oxidation of Met^{144} and Met^{145} near the C-terminus are important sites whose oxidation targets both apo- and calcium-activated CaM for degradation.

Enhanced degradation after leucine substitutions for Met^{144} or Met^{145}

Prior measurements indicate a unique sensitivity to changes within the carboxyl-terminus helix to site-specific mutations and the oxidation of Met^{144} and Met^{145}, which can result in the destabilization of the secondary structure and the structural uncoupling between the opposing domains of CaM (4,28,29,37,38). To understand the contribution of structural perturbations with respect to the recognition and degradation of CaM by the proteasome/Hsp90, we have used site-directed mutagenesis to substitute Met^{144} and/or Met^{145} with leucines, and measured the influence of these mutations on both the secondary structure and rate of degradation by the proteasome/Hsp90. These measurements, made on the CaM-L7 background, indicate that upon mutation of either Met^{144} and/or Met^{145} to Leu that CaM becomes a substrate for degradation by the proteasome/Hsp90 (Fig. 6). However, while mutation of Met^{145} to Leu in the absence of oxidation (i.e., CaM-L8M^{144}) results in the progressive degradation of CaM by the proteasome/Hsp90 (Fig. 6 *A*), the mutation Met^{144} to Leu (i.e., CaM-L8M^{144}) results in a stepwise cleavage of CaM into large fragments that are not subject to further degradation (Fig. 6 *B*). Likewise, the CaM-L9 mutant, in which all nine methionines are mutated to leucines, is cleaved into large fragments by the proteasome/Hsp90. In all cases, cleavage is blocked after proteasome inhibition using either MG132 or epoxomicin (data not shown) as a proteasome inhibitor (Fig. 6), indicating that partial

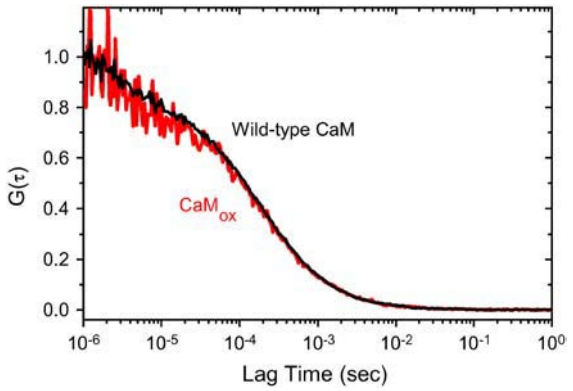

FIGURE 4 Oxidized CaM remains monodisperse in solution. Fluorescence correlation curves for wild-type CaM (*black line*) and after the oxidation of all nine methionines for CaM_{ox} (*red line*), where fits to the data indicate respective translational diffusion coefficients (D_t) of 1.1×10^{-10} $m^2 s^{-1}$ and 1.0×10^{-10} $m^2 s^{-1}$. The expected D_t for CaM (1cll.pdb) is 0.9×10^{-10} $m^2 s^{-1}$ (34). Experimental conditions involve 5 nM Alexa532-labeled CaM in 10 mM MOPS (pH 7.5), 50 mM KCl. Temperature was 25°C. Excitation was 532 nm and emitted light was collected subsequent to a HQ560 emission filters (Chroma Technology).

degradation of CaM-L8M145 is specific to the proteasome rather than a result of the presence of a contaminant protease.

The limited degradation of CaM into several large fragments upon mutation M144L is reminiscent of the cleavage pattern observed for oxidized wild-type CaM, where a similar large fragment of ~10 kDa initially appears and is subsequently degraded (see *inset* in Fig. 1 *A*). Thus, site-specific substitutions at these sites induce a sensitivity to degradation that is qualitatively similar to that associated with the degradation of oxidized wild-type CaM. These observations strengthen earlier suggestions that both Met^{144} and Met^{145} stabilize interhelical contact interactions important to the maintenance of the metastable structure of CaM (28,38) and are consistent with the unique role of the highly linear and flexible methionine side chain that permits efficient stabilization of interfaces through optimal packing interactions (39). Overall, these results indicate a sensitivity to mutations at positions 144 and 145 in helix H near the C-terminus of CaM, which promotes the recognition and degradation of CaM by the proteasome/Hsp90.

CaM degradation and oxidant-induced structural changes

Upon oxidation of Met^{145}, CaM-L8M145 is rapidly and fully degraded by the proteasome/Hsp90 with rates comparable to that associated with fully oxidized wild-type CaM (Fig. 7). In contrast, the site-specific oxidation of Met^{144} does not affect the sensitivity of either apo- or calcium-activated CaM-L8M144 to degradation by the proteasome/Hsp90 (Fig. 7; Table 3). These results indicate that oxidation of Met^{144} does not have a significant effect on the recognition and degradation of CaM_{ox} by the proteasome/Hsp90.

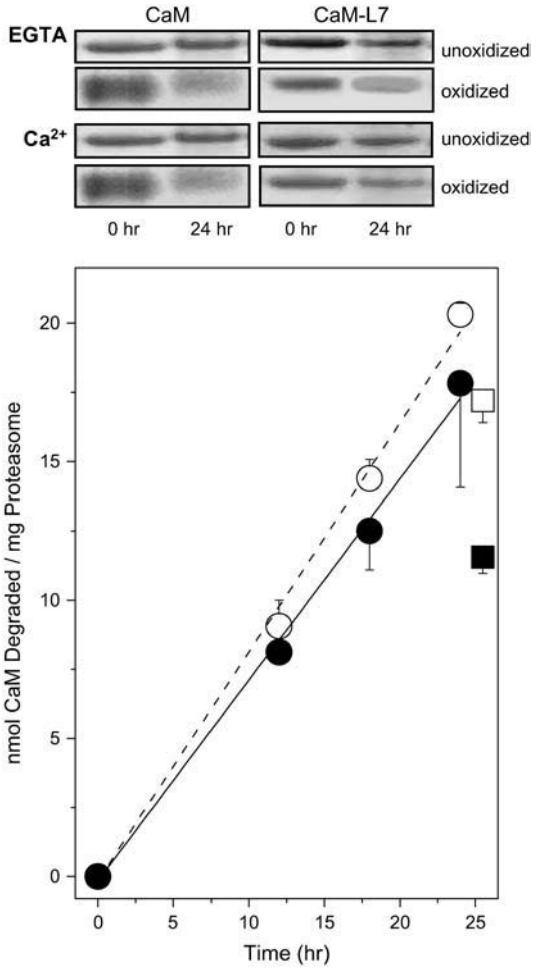

FIGURE 5 Comparable rates of proteolytic digestion for oxidized wild-type and L7-CaM. SDS-PAGE of wild-type CaM or CaM-L7 after incubation for indicated times with 20S proteasome in complex with Hsp90 (*top panel*). The extent of degradation was determined from decreases in the measured band intensity for oxidized CaM in the apo- (○,●) or calcium-activated (□, ■) forms for wild-type CaM (○, □) (*dashed line*) in which all nine methionines were oxidized or (●, ■) CaM-L7 (*solid line*) in which Met^{144} and Met^{145} were selectively oxidized. Experimental points represent the mean and standard deviation of the mean for five replicates. Experimental conditions involved incubation of 15 μM CaM or CaM-L7 at 37°C in the presence of 0.6 μM 20S proteasome and 2.5 μM Hsp90 in 50 mM PIPES (pH 6.5), 0.1 M KCl, 10 mM $MgCl_2$, 2.0 mM ATP, and either 0.1 mM EGTA or 0.1 mM $CaCl_2$.

Using CD spectroscopy to assess possible structural changes associated with the mutation of either Met^{144} or Met^{145} to leucines, we find that the spectral shapes (i.e., $[\Theta_{208}]/[\Theta_{222}]$) (Fig. 7) and thermal stabilities for CaM-L8M144 and CaM-L8M145 are significantly different from each other (Fig. 8). Furthermore, the calculated α-helical content at 37°C for CaM-L8M144 (47% helix) and CaM-L8M145 (40%) is substantially less than wild-type CaM, where there is ~55% helix (14,29,35). In contrast, the substitution of all methionines in CaM with leucines except Met^{144} and Met^{145} (i.e., CaM-L7) has essentially no effect on the secondary structure of CaM (17,35). These results indicate that the site-specific

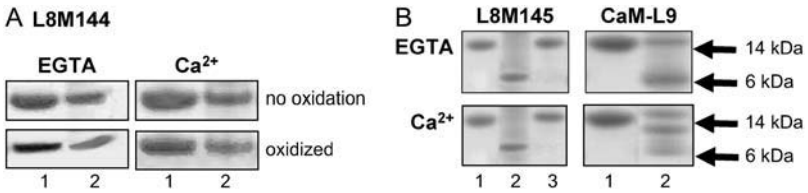

FIGURE 6 Met→Leu substitutions at Met^{144} or Met^{145} induces CaM degradation. SDS-PAGE for apo- and calcium-saturated CaM-L8M144 (*A*), CaM-L8M145 (*B*), and CaM-L9 (*B*), corresponding to initial time-point (lane *1*) and after 24 h incubation with the 20S proteasome/Hsp90 in the absence (lane *2*) or presence (lane *3*) of the proteasome inhibitor MG132 (40 nM). When indicated in panel *A*, Met^{144} was oxidized to its corresponding methionine sulfoxide. Experimental conditions are as described in the legend to Fig. 5. Molecular mass markers are aprotinin (6 kDa) and lysozyme (14 kDa).

substitutions Met144Leu or Met145Leu selectively diminish the helical content of CaM. The observed recognition and partial degradation of these CaM mutants by the proteasome/Hsp90 is, therefore, consistent with prior measurements where oxidant-induced decreases in the helical content of CaM were shown to correlate with its rate of degradation by the proteasome (14). In a complementary experiment, in which only Met^{144} and Met^{145} are mutated to Leu in a wild-type CaM background (i.e., CaM-L2), there is extensive protein aggregation at 37°C, further emphasizing the sensitivity of these amino acids to mutagenesis.

Additional insight regarding the structural transitions associated with the recognition of oxidized CaM for degradation by the proteasome was achieved through a consideration of how the site-specific oxidation of either Met^{144} or Met^{145} in CaM-L8M144 or CaM-L8M145 affects the structure of CaM. The oxidation of Met^{144} in CaM-L8M144 has essentially no effect on the CD spectral shape or thermal stability of CaM, consistent with the observed insensitivity of the oxidation of Met^{144} on the rate of CaM degradation by the proteasome/Hsp90 (Fig. 7). In contrast, the oxidation of Met^{145} significantly perturbs the shape of the CD spectra (i.e., $[\Theta_{208}]/[\Theta_{222}]$) (Fig. 7), indicative of tertiary rather than secondary structural changes. Loss of interhelical contacts would be consistent with subtle tertiary structural changes that facilitate recognition and degradation by the proteasome (Fig. 8) (40). The observed results are in contrast to earlier measurements that have suggested oxidant-induced global unfolding of CaM to promote its degradation by the proteasome (14). Rather, the current results indicate that Met^{145} is a sensitive site whose oxidative modification promotes specific tertiary structural changes that facilitate the recognition and degradation of CaM_{ox} by the proteasome/Hsp90. In contrast, oxidation of Met^{144} has essentially no effect on the susceptibility of CaM to degradation by the proteasome.

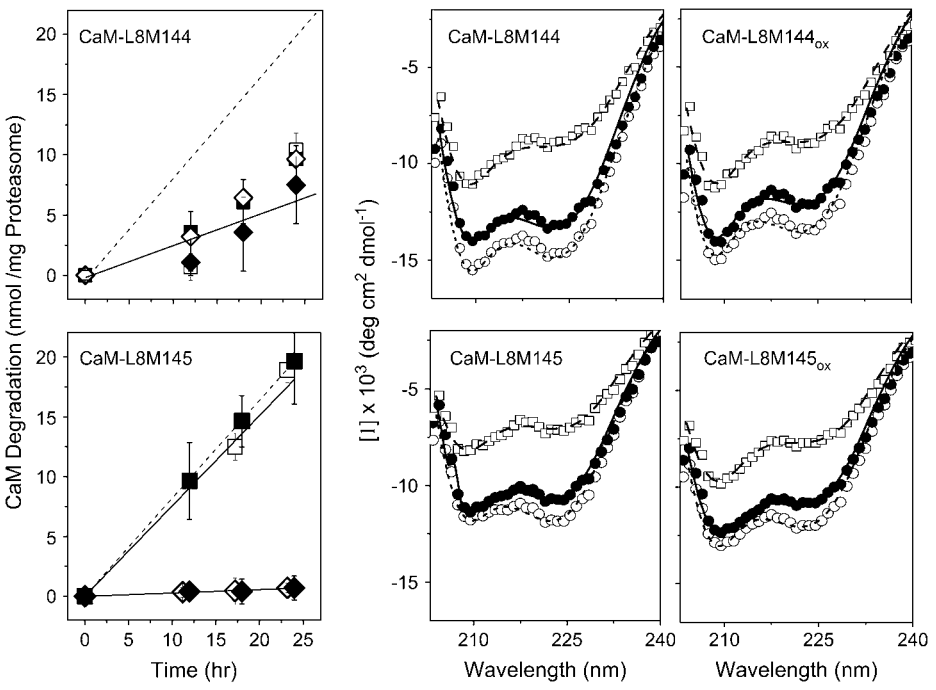

FIGURE 7 CaM degradation and structural effects of methionine oxidation. Rates of proteasomal degradation (*left panels*) and CD spectra (*center* and *right panels*) are shown for CaM-L8M144 (*top*) or CaM-L8M145 (*bottom*). (*Left panels*) Extent of degradation and nonlinear least-squares fits (*solid lines*) before (◇, ◆) or after (□, ■) the oxidation of Met^{144} in CaM-L8M144 (*top*) or Met^{145} in CaM-L8M145 (*bottom*). Dashed lines represent the time-dependent degradation of fully oxidized wild-type CaM (see Fig. 5). Experimental conditions involved incubation of 15 μM calmodulin at 37°C in the presence of 0.6 μM 20S proteasome and 2.5 μM Hsp90 in 50 mM PIPES (pH 6.5), 0.1 M KCl, 10 mM $MgCl_2$, 2.0 mM ATP, and either 0.1 mM EGTA (*open symbols*) or 0.1 mM $CaCl_2$ (*solid symbols*). (*Right panels*) CD spectra were measured at 5°C (○), 35°C (●), and 95°C (□) for CaM (50 μg/ml) in 10 mM Tris (pH 7.5), 50 mM KCl, 1 mM $MgCl_2$, and 0.1 mM $CaCl_2$, and lines represent fits using the program CONTIN (see Experimental Procedures). Experimental points represent the mean and standard errors for five replicates.

TABLE 3 Oxidation-dependent rates of proteasome degradation for CaM mutants

CaM sample		Degradation rate (nmol CaM/mg 20S proteasome/h)	
Nomenclature	Methionines remaining	EGTA	Calcium
CaM_{wt}	36, 51, 71, 72, 76, 109, 124, 144, 145	0.81 ± 0.03	0.68 ± 0.05
CaM-L7	144 and 145	0.40 ± 0.03	0.63 ± 0.04
CaM-L8M144	144	0.00 ± 0.07	0.12 ± 0.04
CaM-L8M145	145	0.72 ± 0.04	0.79 ± 0.04

Experimental conditions are as described in the legend to Fig. 5. Values represent the increased rates of proteasome degradation observed after the homogeneous oxidation of all methionines.

DISCUSSION

Summary

Oxidized CaM is selectively recognized for degradation by the proteasome, resulting in the release of large N-terminal domain fragments (e.g., Ala^{1}–Phe^{92}) and small C-terminus peptides that are highly enriched in Met(O) (Fig. 1 *A*; Table 2). The extent of CaM_{ox} degradation correlates with the stoichiometry of oxidation of the C-terminus tryptic fragment containing Met^{144} and Met^{145} (Fig. 1 *B*), where a similar extent of degradation is apparent irrespective of whether one or both methionines are oxidized (Fig. 2). Since Met^{145} is oxidized before the oxidation of Met^{144} (Fig. 3), these results imply that $Met(O)^{145}$ is a recognition signal that promotes the degradation of CaM_{ox} by the proteasome/Hsp90. Consistent with this observation, we find that the site-specific oxidation of Met^{145} results in comparable rates of proteasomal degradation to that associated with the oxidation of all nine methionines (Fig. 9). Indeed, the site-specific substitution of Leu at this site causes a partial increase in the rate of degradation (Fig. 7, *top left panel*). In contrast, the oxidation of Met^{144} has essentially no effect on the rate of CaM degradation by the proteasome (Fig. 9). Thus, the site-specific oxidation of a single methionine can function to target CaM for degradation by the proteasome, suggesting an important mechanism whereby the targeted oxidative modification of Met^{145} can promote changes in CaM-dependent signaling pathways.

Role of Hsp90 and the 20S proteasome in mediating the degradation of oxidized proteins

Hsp90 copurifies with the 20S proteasome routinely, and functions as a regulatory component to mediate the recognition and degradation of oxidized CaM (15,41–43). Hsp90 in complex with the proteasome selectively recognizes and binds to oxidized CaM (15). Global structural changes associated with the oxidation of CaM primarily arise due to the oxidation of methionines near the carboxyl-terminus (i.e., Met^{144} and Met^{145}), which results in the structural uncoupling between the opposing domains of CaM (28,38). Consistent with a structural role involving the methionines near the carboxyl-terminus, mutation M145L results in the cleavage of CaM into large fragments (Fig. 6). Furthermore, this observation is consistent with the stepwise cleavage of wild-type CaM_{ox} into large fragments observed using mass spectrometry (Fig. 1), which can dissociate and rebind to the proteasome for further degradation (14). The selective recognition and degradation of CaM after the structural disruption associated with either mutations or the oxidation of Met^{145} is, furthermore, consistent with the known role of Hsp90 in mediating the stabilization of ~200 signaling proteins whose structures all contain large amounts of disordered sequence (44–46). The preferential recognition and targeting of disordered proteins (such as CaM_{ox}) by Hsp90 for degradation by the proteasome has important implications whereby unfolded signaling proteins are rapidly targeted for degradation, and has the potential to rapidly decrease the abundance of CaM and other critical regulatory proteins in response to oxidative stress.

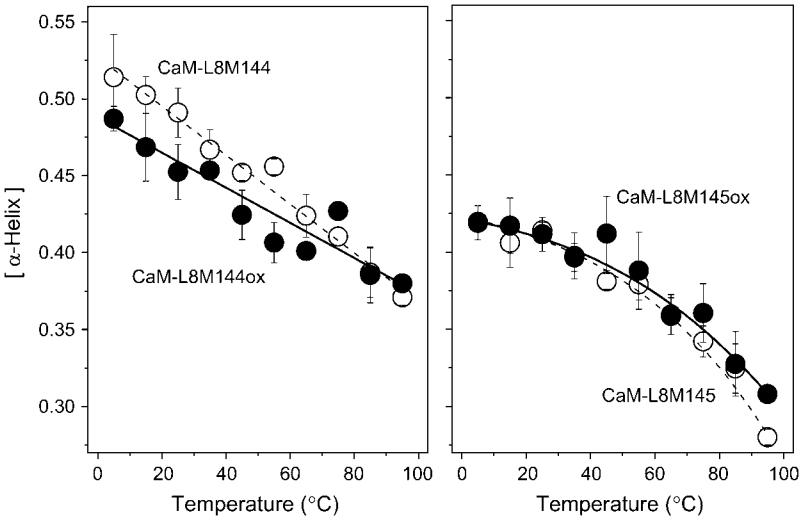

FIGURE 8 Calculated α-helical content using the program CONTINLL before (○) and after (●) oxidation of single methionine for CaM-L8M144 (*left panel*) or CaM-L8M145 (*right panel*) in 10 mM Tris (pH 7.5), 50 mM KCl, 1 mM $MgCl_2$, and 0.1 mM $CaCl_2$.

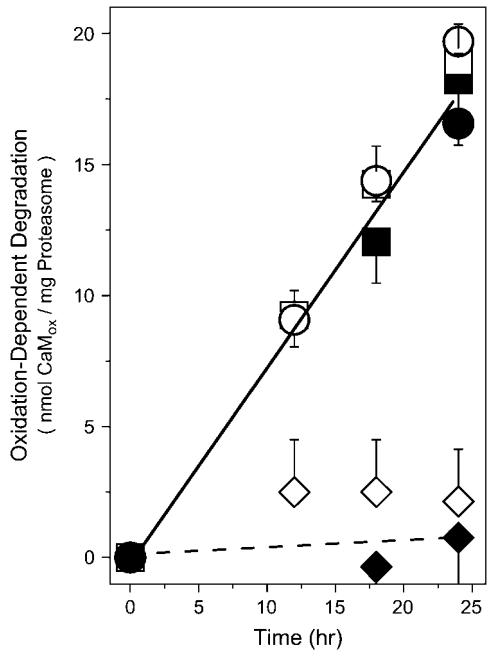

FIGURE 9 Summary of oxidation-dependent degradation of CaM_{ox} by the proteasome. The extent of degradation at indicated time-points is shown for wild-type CaM (○,●); CaML8-M144 (◇,◆); and CaML8-M145 (□,■) in the apo- (○,◇,□) or calcium-activated (●,◆,■) forms. Experimental conditions are as described in legend to Fig. 5.

Mechanisms underlying CaM expression and turnover

The cellular abundance of CaM is tightly regulated, since 1), target proteins are in excess of available CaM; and 2), changes in the total amount of cellular CaM relative to target proteins functions to coordinate cellular metabolism (2,47). Indeed, mitogenic stimulation with insulin functions to increase CaM expression levels and upregulate cellular metabolism through the selected activation of critical transcription factors such as Sp1 (48–50). Likewise, cellular CaM levels are rapidly upregulated upon macrophage activation (51). Increases in CaM expression levels result in sustained levels of cellular activation, with the return to the basal metabolic state requiring the sequestration or degradation of excess CaM. In this latter respect, CaM has been shown to be degraded in a ubiquitin-independent process involving the proteasome with a half-life of ~18 h (7,52). However, the signals that target CaM for degradation by the proteasome have remained unclear. Recent results, demonstrating a role for Hsp90 in association with the 20S proteasome in mediating the recognition and degradation of oxidized CaM, suggest that this complex plays an important role in the modulation of cellular signaling (15). Indeed, physiological regulation of proteasome activity appears to be modulated by a dynamic equilibrium between different forms of the multiprotein complex, in which the catalytic 20S core proteasome is present alone or in complex with other protein complexes in addition to Hsp90, including the 19S regulatory complex (PA700) and 11S REG (PA28). Thus, under conditions of oxidative stress and the associated increase in the expression levels of Hsp90, proteasomal degradation may be shifted toward the selective recognition and degradation of oxidized proteins, including CaM_{ox}, as an alternative to repair by endogenous methionine sulfoxide reductases (4).

The mechanism of CaM_{ox} degradation involves binding to Hsp90 and cleavage by the 20S proteasome. Degradation is nonprocessive, with the initial cleavage of oxidized CaM into large fragments that are apparent using mass spectrometry (Fig. 1), which can then dissociate and rebind with the proteasome for further degradation (14). Indeed, the substitution Met144Leu induces proteasomal cleavage and the release of a large fragment that is similar to that observed for CaM_{ox} (Figs. 1 *A* and 6). The observation of a similar CaM fragment using either wild-type CaM (Fig. 1 *A*) or a CaM mutant in which the majority of methionines are substituted with leucines (i.e., CaM-L8M145; see Fig. 6 *B*) provides confidence that CaM is recognized and degraded in a stepwise manner by the proteasome upon modification of Met^{144} or Met^{145}. These results suggest the 20S proteasome initially cleaves targeted sites after recognition and binding of CaM by Hsp90, and that, after cleavage, CaM fragments can dissociate from the proteasome complex (Fig. 10). However, under conditions where Met^{145} is oxidized, the rebinding and degradation of CaM fragments occurs and large

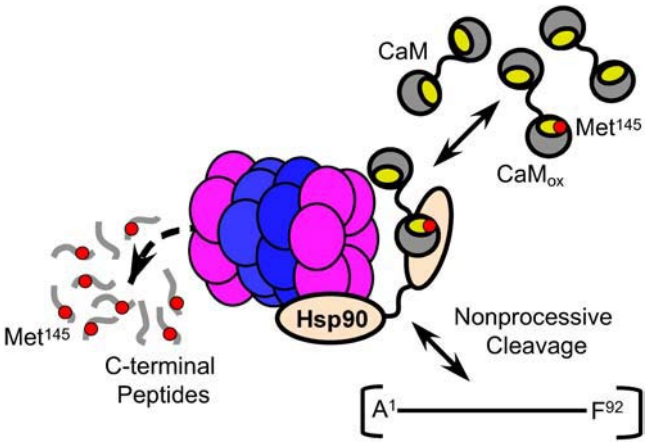

FIGURE 10 Model highlighting role of Met^{145} as a sensor in mediating recognition and degradation of CaM_{ox} by proteasome. The 20S proteasome complex composed of rings of α- (*purple*) and β- (*blue*) subunits in association with Hsp90 oligomers (*tan*) preferentially recognizes and degrades CaM_{ox} after oxidation of Met^{145} to its sulfoxide (*red dot*). CaM_{ox} containing Met^{145} in hydrophobic binding pocket (*yellow*) is targeted for degradation; intermediates indicative of the nonprocessive cleavage of CaM_{ox} include large fragments A^1-F^{89} (not shown) and A^1-F^{92} as well as C-terminus peptides (G^{132}–K^{148}) enriched in $Met(O)^{145}$. Similar intermediates involving large CaM fragments are observed upon site-directed substitution of Met^{144} and Met^{145} with leucines (Fig. 6), consistent with a structural sensitivity at positions 144 or 145.

fragments do not accumulate (Fig. 7). These latter results suggest a kinetic balance between the release of CaM_{ox} from Hsp90 and its relative rate of entry and degradation by the 20S proteasome. Since the proteasome has a relatively low turnover number, the release of CaM_{ox} following targeted proteolysis would permit the rapid recognition and inactivation of CaM_{ox} that would function to diminish its cellular abundance. Thus, there may be a kinetic balance between rates of CaM_{ox} repair by endogenous methionine sulfoxide reductases (Msr) and the degradation by the proteasome that is modulated by cellular redox conditions associated with the regulation of Msr function and cellular calcium levels as well as the abundance of Hsp90 that affects the amount of 20S proteasome relative to its other forms.

Oxidative stress and cellular signaling

Reactive oxygen species can function as second messengers through the oxidation of key regulatory proteins, resulting in either altered function or targeted degradation. In the case of CaM, the selective oxidation of Met^{145} results in recognition and degradation by the proteasome (Fig. 9). Oxidation of this surface-exposed residue is functionally distinct from the oxidation of other methionines, including Met^{144}, which results in the modulation of target protein function (17,36). Furthermore, the sensitivity of Met^{145} to oxidation is highly dependent on the source of reactive oxygen species and the surrounding sequence in different CaM isoforms (21,53,54). For example, Met^{145} is differentially oxidized by hydrogen peroxide and peroxynitrite, providing a differential cellular readout that is dependent on the source of oxidative stress. Likewise, the much greater sensitivity of plant CaM to the oxidation of Met^{145}, whose sequence differs primarily in the vicinity of Met^{144} and Met^{145}, may function as part of an adaptive cellular mechanism that permits increased responsiveness to oxidative stress. These results argue that Met^{145} functions, in part, as a sensor of oxidative stress to modulate the rate of CaM turnover by the proteasome.

Site-specific differences in the function of CaM resulting from the differential oxidation of Met^{144} and Met^{145} have previously been observed. For example, prior results indicate that the oxidation of Met^{144} is primarily responsible for the nonproductive binding of CaM_{ox} to target enzymes (i.e., the plasma membrane Ca-ATPase) that stabilize the inhibited state (17,27,55), suggesting a functional dichotomy where the site-specific oxidation of individual methionines can promote either proteasomal degradation or enzyme inhibition. These differences may have important physiological implications relating to the sensitivities of these sites to oxidative modification, as molecular dynamics calculations indicate that the sulfur atoms in Met^{144} and Met^{145} have very different surface accessibilities; the surface accessibility of Met^{145} is $\sim$25 $Å^2$ while the surface accessibility of Met^{144} is close to zero (21). Surface-exposed residues are preferentially oxidized by long-lived species such as hydrogen peroxide, while alternate sites (including Met^{144}) are oxidized by highly reactive species such as peroxynitrite (53). Thus, the site-specific oxidation of specific methionines in CaM by reactive oxygen species with differing selectivities have the potential to couple different oxidative stressors to cellular signaling cascades through the modulation of CaM function and expression levels.

Conclusions and future directions

We have demonstrated a key role for the site-specific oxidation of a single methionine (i.e., Met^{145}) in modulating the recognition and turnover of CaM by the proteasome. Since the abundance of CaM regulates cell function through the modulation of cellular metabolism and transcriptional regulation, these results provide an important example of the selective degradation of a critical signaling molecule using methionine oxidization as a sensor of oxidative stress. Furthermore, senescent brain shows an accumulation of oxidized CaM that contains multiple methionine sulfoxides but lacks significant oxidation at Met^{145}, which is consistent with a role for methionine oxidation in modulating the degradation of CaM by the proteasome (5,21). Future measurements should extend these observations to examine the consequences of changes in CaM expression levels on cellular signaling cascades through a consideration of changes in binding partners, and the importance of this degradation pathway on cellular metabolism.

This work was supported by grants from the National Institutes of Health (No. AG12993 and No. AG17996). Pacific Northwest National Laboratory is operated for the Department of Energy by Battelle Memorial Institute under contract No. DEAC05-76RLO 1830. A portion of the research described in this article was performed in the Environmental Molecular Sciences Laboratory, a National Scientific User Facility sponsored by Department of Energy's Office of Biological and Environmental Research and located at Pacific Northwest National Laboratory.

REFERENCES

1. Yap, K. L., J. Kim, K. Truong, M. Sherman, T. Yuan, and M. Ikura. 2000. Calmodulin target database. *J. Struct. Funct. Genomics.* 1:8–14.
2. Tran, Q. K., D. J. Black, and A. Persechini. 2003. Intracellular coupling via limiting calmodulin. *J. Biol. Chem.* 278:24247–24250.
3. Persechini, A., and P. M. Stemmer. 2002. Calmodulin is a limiting factor in the cell. *Trends Cardiovasc. Med.* 12:32–37.
4. Bigelow, D. J., and T. C. Squier. 2005. Redox modulation of cellular signaling and metabolism through reversible oxidation of methionine sensors in calcium regulatory proteins. *Biochim. Biophys. Acta.* 1703: 121–134.
5. Gao, J., D. Yin, Y. Yao, T. D. Williams, and T. C. Squier. 1998. Progressive decline in the ability of calmodulin isolated from aged brain to activate the plasma membrane Ca-ATPase. *Biochemistry.* 37:9536–9548.
6. Lu, T., Y. Pan, S. Y. Kao, C. Li, I. Kohane, J. Chan, and B. A. Yankner. 2004. Gene regulation and DNA damage in the ageing human brain. *Nature.* 429:883–891.
7. Tarcsa, E., G. Szymanska, S. Lecker, C. M. O'Connor, and A. L. Goldberg. 2000. Ca^{2+}-free calmodulin and calmodulin damaged by in

vitro aging are selectively degraded by 26S proteasomes without ubiquitination. *J. Biol. Chem.* 275:20295–20301.

8. Davies, K. J. 2001. Degradation of oxidized proteins by the 20S proteasome. *Biochimie*. 83:301–310.
9. Benaroudj, N., E. Tarcsa, P. Cascio, and A. L. Goldberg. 2001. The unfolding of substrates and ubiquitin-independent protein degradation by proteasomes. *Biochimie*. 83:311–318.
10. Hoyt, M. A., and P. Coffino. 2004. Ubiquitin-free routes into the proteasome. *Cell. Mol. Life Sci.* 61:1596–1600.
11. Hochstrasser, M. 1996. Protein degradation or regulation: Ub the judge. *Cell*. 84:813–815.
12. Majetschak, M., M. Laub, H. E. Meyer, and H. P. Jennissen. 1998. The ubiquityl-calmodulin synthetase system from rabbit reticulocytes: isolation of the ubiquitin-binding first component, a ubiquitin-activating enzyme. *Eur. J. Biochem.* 255:482–491.
13. Laub, M., J. A. Steppuhn, M. Bluggel, D. Immler, H. E. Meyer, and H. P. Jennissen. 1998. Modulation of calmodulin function by ubiquitin-calmodulin ligase and identification of the responsible ubiquitylation site in vertebrate calmodulin. *Eur. J. Biochem.* 255:422–431.
14. Ferrington, D. A., H. Sun, K. K. Murray, J. Costa, T. D. Williams, D. J. Bigelow, and T. C. Squier. 2001. Selective degradation of oxidized calmodulin by the 20S proteasome. *J. Biol. Chem.* 276:937–943.
15. Whittier, J. E., Y. Xiong, M. C. Rechsteiner, and T. C. Squier. 2004. Hsp90 enhances degradation of oxidized calmodulin by the 20S proteasome. *J. Biol. Chem.* 279:46135–46142.
16. Galeva, N. A., S. W. Esch, T. D. Williams, L. M. Markille, and T. C. Squier. 2005. Rapid method for quantifying the extent of methionine oxidation in intact calmodulin. *J. Am. Soc. Mass Spectrom.* 16:1470–1480.
17. Bartlett, R. K., R. J. Bieber Urbauer, A. Anbanandam, H. S. Smallwood, J. L. Urbauer, and T. C. Squier. 2003. Oxidation of Met^{144} and Met^{145} in calmodulin blocks calmodulin-dependent activation of the plasma membrane Ca-ATPase. *Biochemistry*. 42: 3231–3238.
18. Strasburg, G. M., M. Hogan, W. Birmachu, D. D. Thomas, and C. F. Louis. 1988. Site-specific derivatives of wheat germ calmodulin. Interactions with troponin and sarcoplasmic reticulum. *J. Biol. Chem.* 263:542–548.
19. Hoffman, L., G. Pratt, and M. Rechsteiner. 1992. Multiple forms of the 20S multicatalytic and the 26S ubiquitin/ATP-dependent proteases from rabbit reticulocyte lysate. *J. Biol. Chem.* 267:22362–22368.
20. Dubiel, W., G. Pratt, K. Ferrell, and M. Rechsteiner. 1992. Purification of an 11S regulator of the multicatalytic protease. *J. Biol. Chem.* 267: 22369–22377.
21. Yin, D., K. Kuczera, and T. C. Squier. 2000. The sensitivity of carboxyl-terminal methionines in calmodulin isoforms to oxidation by H_2O_2 modulates the ability to activate the plasma membrane Ca-ATPase. *Chem. Res. Toxicol.* 13:103–110.
22. Klee, C. B., and T. C. Vanaman. 1982. Calmodulin. *Adv. Protein Chem.* 35:213–321.
23. Nelson, D. P., and L. A. Kiesow. 1972. Enthalpy of decomposition of hydrogen peroxide by catalase at 25°C (with molar extinction coefficients of H_2O_2 solutions in the UV). *Anal. Biochem.* 49:474–478.
24. Shen, Y., R. Zhao, M. E. Belov, T. P. Conrads, G. A. Anderson, K. Tang, L. Pasa-Tolic, T. D. Veenstra, M. S. Lipton, H. R. Udseth, and R. D. Smith. 2001. Packed capillary reversed-phase liquid chromatography with high-performance electrospray ionization Fourier transform ion cyclotron resonance mass spectrometry for proteomics. *Anal. Chem.* 73:1766–1775.
25. Horn, D. M., R. A. Zubarev, and F. W. McLafferty. 2000. Automated reduction and interpretation of high resolution electrospray mass spectra of large molecules. *J. Am. Soc. Mass Spectrom.* 11:320–332.
26. Sreerama, N., and R. W. Woody. 2000. Estimation of protein secondary structure from circular dichroism spectra: comparison of CONTIN, SELCON, and CDSSTR methods with an expanded reference set. *Anal. Biochem.* 287:252–260.
27. Yao, Y., D. Yin, G. S. Jas, K. Kuczer, T. D. Williams, C. Schoneich, and T. C. Squier. 1996. Oxidative modification of a carboxyl-terminal vicinal methionine in calmodulin by hydrogen peroxide inhibits calmodulin-dependent activation of the plasma membrane Ca-ATPase. *Biochemistry*. 35:2767–2787.
28. Gao, J., Y. Yao, and T. C. Squier. 2001. Oxidatively modified calmodulin binds to the plasma membrane Ca-ATPase in a nonproductive and conformationally disordered complex. *Biophys. J.* 80: 1791–1801.
29. Gao, J., D. H. Yin, Y. Yao, H. Sun, Z. Qin, C. Schoneich, T. D. Williams, and T. C. Squier. 1998. Loss of conformational stability in calmodulin upon methionine oxidation. *Biophys. J.* 74:1115–1134.
30. Chen, B., M. U. Mayer, and T. C. Squier. 2005. Structural uncoupling between opposing domains of oxidized calmodulin underlies the enhanced binding affinity and inhibition of the plasma membrane Ca-ATPase. *Biochemistry*. 44:4737–4747.
31. Grune, T., T. Reinheckel, and K. J. Davies. 1996. Degradation of oxidized proteins in K562 human hematopoietic cells by proteasome. *J. Biol. Chem.* 271:15504–15509.
32. Grune, T., K. Merker, G. Sandig, and K. J. Davies. 2003. Selective degradation of oxidatively modified protein substrates by the proteasome. *Biochem. Biophys. Res. Commun.* 305:709–718.
33. Hess, S. T., S. Huang, A. A. Heikal, and W. W. Webb. 2002. Biological and chemical applications of fluorescence correlation spectroscopy: a review. *Biochemistry*. 41:697–705.
34. Garcia De La Torre, J., M. L. Huertas, and B. Carrasco. 2000. Calculation of hydrodynamic properties of globular proteins from their atomic-level structure. *Biophys. J.* 78:719–730.
35. Anbanandam, A., R. J. Bieber Urbauer, R. K. Bartlett, H. S. Smallwood, T. C. Squier, and J. L. Urbauer. 2005. Mediating molecular recognition by methionine oxidation: conformational switching by oxidation of methionine in the carboxyl-terminal domain of calmodulin. *Biochemistry*. 44:9486–9496.
36. Montgomery, H. J., R. Bartlett, B. Perdicakis, E. Jervis, T. C. Squier, and J. G. Guillemette. 2003. Activation of constitutive nitric oxide synthases by oxidized calmodulin mutants. *Biochemistry*. 42: 7759–7768.
37. Yin, D., H. Sun, D. A. Ferrington, and T. C. Squier. 2000. Closer proximity between opposing domains of vertebrate calmodulin following deletion of Met^{145}–Lys^{148}. *Biochemistry*. 39:10255–10268.
38. Sun, H., D. Yin, L. A. Coffeen, M. A. Shea, and T. C. Squier. 2001. Mutation of Tyr^{138} disrupts the structural coupling between the opposing domains in vertebrate calmodulin. *Biochemistry*. 40: 9605–9617.
39. Gellman, S. H. 1991. On the role of methionine residues in the sequence-independent recognition of nonpolar protein surfaces. *Biochemistry*. 30:6633–6636.
40. Dong, M., L. Ladaviere, F. Penin, G. Deleage, and L. G. Baggetto. 1998. Secondary structure of P-glycoprotein investigated by circular dichroism and amino acid sequence analysis. *Biochim. Biophys. Acta.* 1371:317–334.
41. Conconi, M., I. Petropoulos, I. Emod, E. Turlin, F. Biville, and B. Friguet. 1998. Protection from oxidative inactivation of the 20S proteasome by heat-shock protein 90. *Biochem. J.* 333:407–415.
42. Montel, V., F. Gardrat, J. L. Azanza, and J. Raymond. 1999. 20S proteasome, Hsp90, p97 fusion protein, PA28 activator copurifying oligomers and ATPase activities. *Biochem. Mol. Biol. Int.* 47: 465–472.
43. Wagner, B. J., and J. W. Margolis. 1995. Age-dependent association of isolated bovine lens multicatalytic proteinase complex (proteasome) with heat-shock protein 90, an endogenous inhibitor. *Arch. Biochem. Biophys.* 323:455–462.
44. Iakoucheva, L. M., C. J. Brown, J. D. Lawson, Z. Obradovic, and A. K. Dunker. 2002. Intrinsic disorder in cell-signaling and cancer-associated proteins. *J. Mol. Biol.* 323:573–584.
45. Vucetic, S., Z. Obradovic, V. Vacic, P. Radivojac, K. Peng, L. M. Iakoucheva, M. S. Cortese, J. D. Lawson, C. J. Brown, J. G. Sikes,

C. D. Newton, and A. K. Dunker. 2005. DisProt: a database of protein disorder. *Bioinformatics.* 21:137–140.

46. Young, J. C., I. Moarefi, and F. U. Hartl. 2001. Hsp90: a specialized but essential protein-folding tool. *J. Cell Biol.* 154:267–273.
47. Taylor, J. E., M. R. McAinsh, L. Montgomery, K. F. Renwick, A. A. Webb, and A. M. Hetherington. 1994. The use of transgenesis to investigate signal-transduction pathways. *Biochem. Soc. Trans.* 22: 949–952.
48. Keembiyehetty, C. N., R. P. Candelaria, G. Majumdar, R. Raghow, A. Martinez-Hernandez, and S. S. Solomon. 2002. Paradoxical regulation of Sp1 transcription factor by glucagon. *Endocrinology.* 143: 1512–1520.
49. Majumdar, G., A. Harmon, R. Candelaria, A. Martinez-Hernandez, R. Raghow, and S. S. Solomon. 2003. O-glycosylation of Sp1 and transcriptional regulation of the calmodulin gene by insulin and glucagon. *Am. J. Physiol. Endocrinol. Metab.* 285:E584–E591.
50. Navarrete Santos, A., S. Tonack, M. Kirstein, M. Pantaleon, P. Kaye, and B. Fischer. 2004. Insulin acts via mitogen-activated protein kinase phosphorylation in rabbit blastocysts. *Reproduction.* 128:517–526.
51. Weber, T. J., H. S. Smallwood, L. E. Kathmann, L. M. Markillie, T. C. Squier, and B. D. Thrall. 2006. Functional linkage between tumor necrosis factor biosynthesis and calmodulin-dependent activation of iNOS in RAW 264.7 macrophages. *Am. J. Physiol. Cell. Physiol.* 2906:C1512–C1520.
52. Ferrington, D. A., X. Chen, A. G. Krainev, E. K. Michaelis, and D. J. Bigelow. 1997. Protein half-lives of calmodulin and the plasma membrane Ca-ATPase in rat brain. *Biochem. Biophys. Res. Commun.* 237:163–165.
53. Squier, T. C., and D. J. Bigelow. 2000. Protein oxidation and age-dependent alterations in calcium homeostasis. *Front. Biosci.* 5: D504–D526.
54. Huhmer, A. F., N. C. Gerber, P. R. de Montellano, and C. Schoneich. 1996. Peroxynitrite reduction of calmodulin stimulation of neuronal nitric oxide synthase. *Chem. Res. Toxicol.* 9:484–491.
55. Osborn, K. D., R. K. Bartlett, A. Mandal, A. Zaidi, R. J. Urbauer, J. L. Urbauer, N. Galeva, T. D. Williams, and C. K. Johnson. 2004. Single-molecule dynamics reveal an altered conformation for the auto-inhibitory domain of plasma membrane Ca^{2+}-ATPase bound to oxidatively modified calmodulin. *Biochemistry.* 43:12937–12944.